Int. J. Plasma Environ. Sci. Technol. 17 (2023) e01002 (12pp)
International Journal of Plasma Environmental Science and Technology

*Regular Paper* DOI: 10.34343/ijpest.2023.17.e01002

# Superheated steam decomposition by atmospheric pressure plasma

**Muhd Hadi Iskandar*, Yukio Hayakawa, Shinji Kambara**

Graduate School of Engineering, Gifu University, Japan

* Corresponding author: a3921019@edu.gifu-u.ac.jp (Muhd Hadi Iskandar)

Received: 21 October 2022
Revised: 22 January 2023
Accepted: 29 January 2023
Published online: 31 January 2023

## Abstract

Water is being considered as a source material for hydrogen production due to its abundance in nature. This can lead to promising replacements in terms of hydrogen storage and transport. In this study, saturated and superheated steam has been decomposed using a cylindrical type plasma reactor and atmospheric pressure plasma. Steam, in its superheated state, has advantageous properties in increasing plasma decomposition efficiency compared to saturated steam. Hydrogen production has been found dependent on the supplied steam flow rate, residence time, applied voltage and steam temperature. The hydrogen generation rate has shown to increase by up to 1.5 times by increasing the residence time by 17 ms. Superheated steam temperature of up to 300°C has been investigated. Results show that increasing the steam temperature has led to increased hydrogen production activity. Increasing the steam temperature from 100°C to 300°C has shown to almost double the hydrogen generation rate under the same experimental conditions.
.

**Keywords:** Superheated steam, hydrogen production, atmospheric pressure plasma, DBD plasma.

## 1. Introduction

As the world faces unprecedented energy challenges, many countries are looking to include smart energy solutions as an effort to reach a sustainable future [1–4]. One such effort is reducing the use of fossil fuels to generate energy for daily use [5–6]. Hydrogen energy is perceived as an ideal candidate to solve the energy and environmental crisis, and its use in fuel-cell vehicle is especially promising [7–10]. However, for the development of a hydrogen economy, it is important to have a hydrogen generation process that can produce hydrogen efficiently at a cost comparable to that of fossil fuels [11–13]. Currently, 80-85% of the world's hydrogen is produced through steam methane reforming. This process utilizes fossil fuel and emits greenhouse gases, which has dangerous effects on the environment. One alternative method is using water vapor plasmolysis, which is the dissociation of water into hydrogen and oxygen through collision of electrons by plasma energy, and a potentially advantageous and cleaner method of producing hydrogen [14–16]. However, the problem with such alternative method is that it often results in low hydrogen generation efficiency [17–18].

Gas discharge plasma can be classified into thermal and nonthermal equilibrium plasmas. Dielectric barrier discharge plasma is a nonthermal equilibrium plasma with extremely high electron temperature but ambient temperature gas [19]. Dielectric barrier discharges are generated when a dielectric material is placed on one of the electrodes with an AC or pulse voltage being applied between the electrodes [20]. Atmospheric pressure plasma generated by dielectric barrier discharge has the ability to decompose substances using high electron energy, such as decomposition of ammonia gas to obtain hydrogen [21–24]. Similarly, it is also possible to obtain hydrogen through discharge decomposition of water with atmospheric pressure plasma [25–26]. However, it is difficult to decompose water in its liquid state as too many atoms and molecules colliding with electrons will result in them not being ionized or dissociating, but only excited. Therefore, it is better to convert water in the form of steam instead before being decomposed by atmospheric pressure plasma [27].

Industrial heat waste is often generated in large amounts and is released into the environment even after heat recovery processes have been applied. The overall waste heat accounts for nearly a third of the total energy consumed. In order to maximize efficiency and to avoid energy loss in factories and industrial sectors, waste heat is often reused for reheating or preheating through the use of heat exchanger and cooling through a thermo-driven refrigeration system [28–29]. Industrial waste heat potential is limited for temperatures over 1000°C and is only observed in the iron and steel industries. As can be seen in Fig. 1, there is not much waste heat available in the 500-1000°C while heat waste potential is limited to pulp and paper industry in the 200-500°C range [30]. Majority of heat waste often lies in the 100-200°C range, spreading over most industrial sectors. Since its low temperature often leads to low conversion efficiency, waste heat for 100-200°C range is hardly reused to generate power by traditional methods. It can however be used as a heat source for heating water to superheated temperatures instead [31–34].

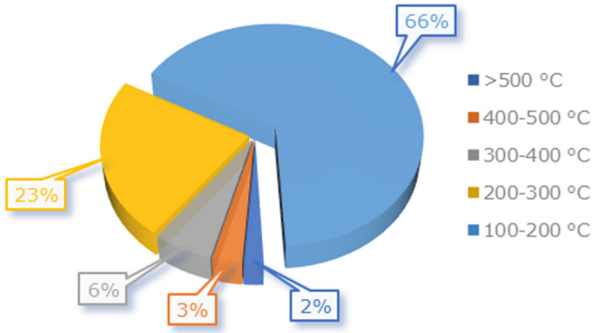


**Fig. 1.** Majority of heat waste from industries ranges from 100°C to 200°C.

Superheated steam refers to the state of steam with a temperature higher than the boiling point and exists as a gaseous water state, where it behaves both as dry hot gas and as steam [35–36]. Fig. 2 shows the superheated generation process. While water turns into steam at 100°C simply by boiling, superheated steam is generated in two stages. Water is first heated to its boiling point and is evaporated to produce saturated steam; further heating with temperatures above the boiling point at a corresponding pressure converts the saturated steam to superheated steam. Superheated steam has the characteristics of having high thermal energy and can exist at high temperature at normal pressure. Superheated steam also has high thermal conductivity and is less likely to condense to liquid compared to saturated steam. Unlike saturated steam which condenses when there is a drop in temperature, superheated steam is much more resistant to condensation so long as temperature is maintained above saturation temperature at a specific pressure. These features are advantageous as having high thermal energy results in easier decomposition compared to saturated steam [37–38]. In addition, it is better for superheated steam to maintain its vapor/gaseous state as liquid would inhibit plasma firing. Water vapor density is also higher as the amount of air contained in steam is lower in low oxygen conditions, resulting in higher plasma decomposition efficiency.

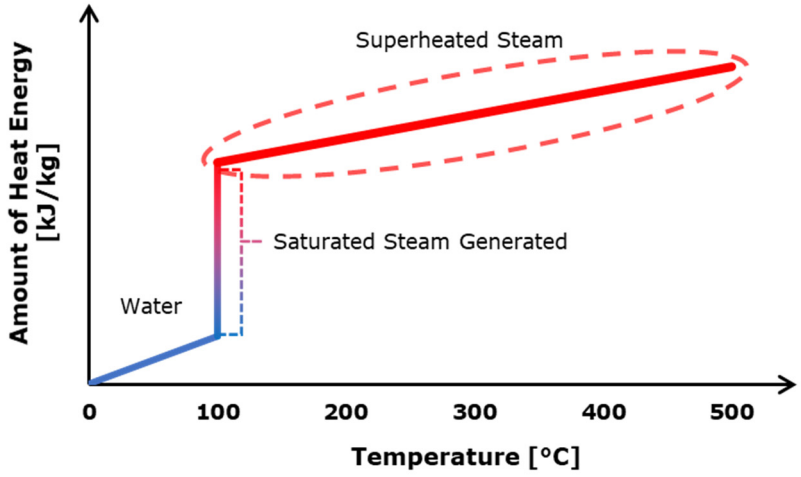


**Fig. 2.** Superheated steam generation process [39].

The purpose of this study is to investigate the decomposition of steam for hydrogen generation in a plasma reactor. This paper reports the characteristics of hydrogen generation from saturated steam and superheated steam using atmospheric pressure plasma.

## 2. Experimental

Fig. 3 below shows the experimental setup for steam decomposition by atmospheric pressure plasma. The experimental setup consists of an electric boiler (Nihon Dennetsu, Boiler V), heating furnace (Asahi Rika Seisakusho Co, ARFLC-50KC), heating oven (Yamato Scientific CO. Ltd, DVS402), a cylindrical type plasma reactor (CPR), a high-voltage pulse power supply, an ice trap, ribbon heater, a displacement tank, and gas chromatograph machine. The CPR (Fig. 4) consists of a main body made of SUS 304 and is encased coaxially within a quartz glass tube which acts as the dielectric material. The reaction zone is the area where the glass tube is wrapped with a sheet of conducting foil which is then fastened together with strips of punching metal. The reactor has an overall length of 180 mm and a reaction zone of 100 mm. The difference between the outer diameter of the SUS tube and the inner diameter of the glass tube is measured as the gap length of the reactor.

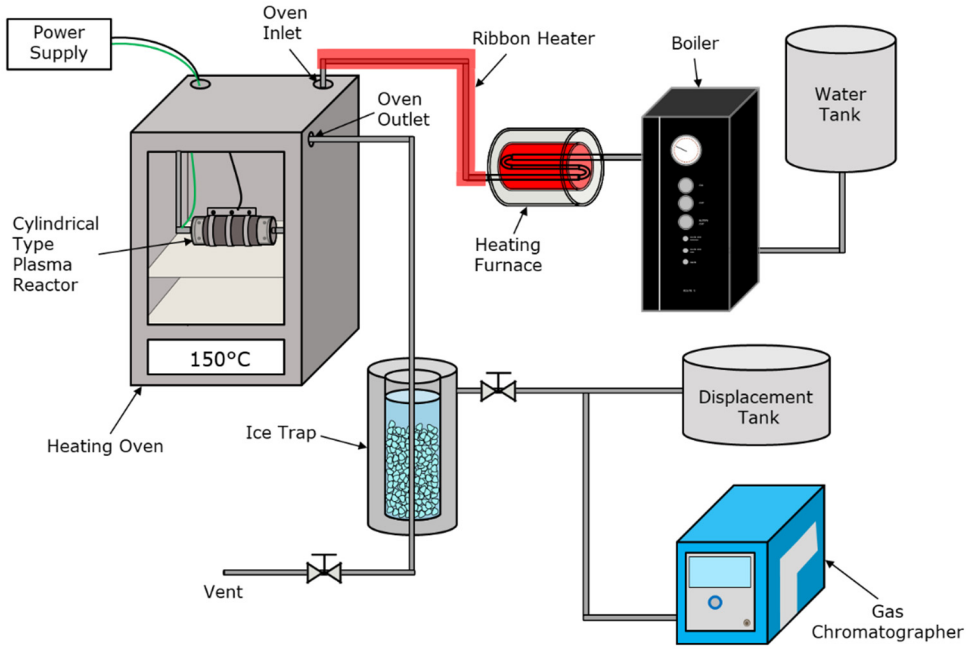


**Fig. 3.** Experimental setup for steam decomposition by cylindrical type plasma reactor.

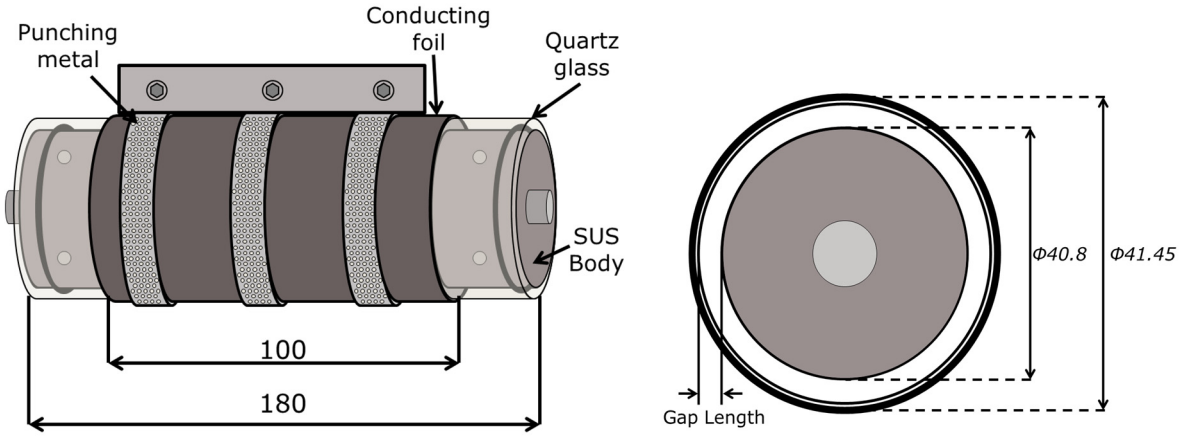


**Fig. 4.** Schematic diagram of cylindrical type plasma reactor.

In this work, the reactor gap length used were measured as 0.325 mm and 0.400 mm. Atmospheric pressure plasma is generated within the reaction gap between the conducting foil which acts as a high voltage electrode and the main body of the reactor which acts as the ground electrode and is generated using a high frequency and high-voltage pulse power supply (Haiden Laboratory, PHF-2K Type) with a waveform shown in Fig. 5. This power supply has an output voltage of 0 to ± 15 $kV_{pp}$, an output capacitance of 0.5 to 2 kW and an output frequency of 1 to 100 kHz. A high voltage probe (Tektronix. P6015A) and an oscilloscope (Tektronix, TDS3034B) were used to measure the waveform. The pulse frequency was kept constant at 10 kHz. The applied voltage ($V_{PP}$) is defined as the voltage between the positive and negative peaks on the oscilloscope.

In this research, the decomposition characteristics of superheated steam using atmospheric pressure plasma was investigated based on a hydrogen generation experiment that used ammonia as source material [40–41].

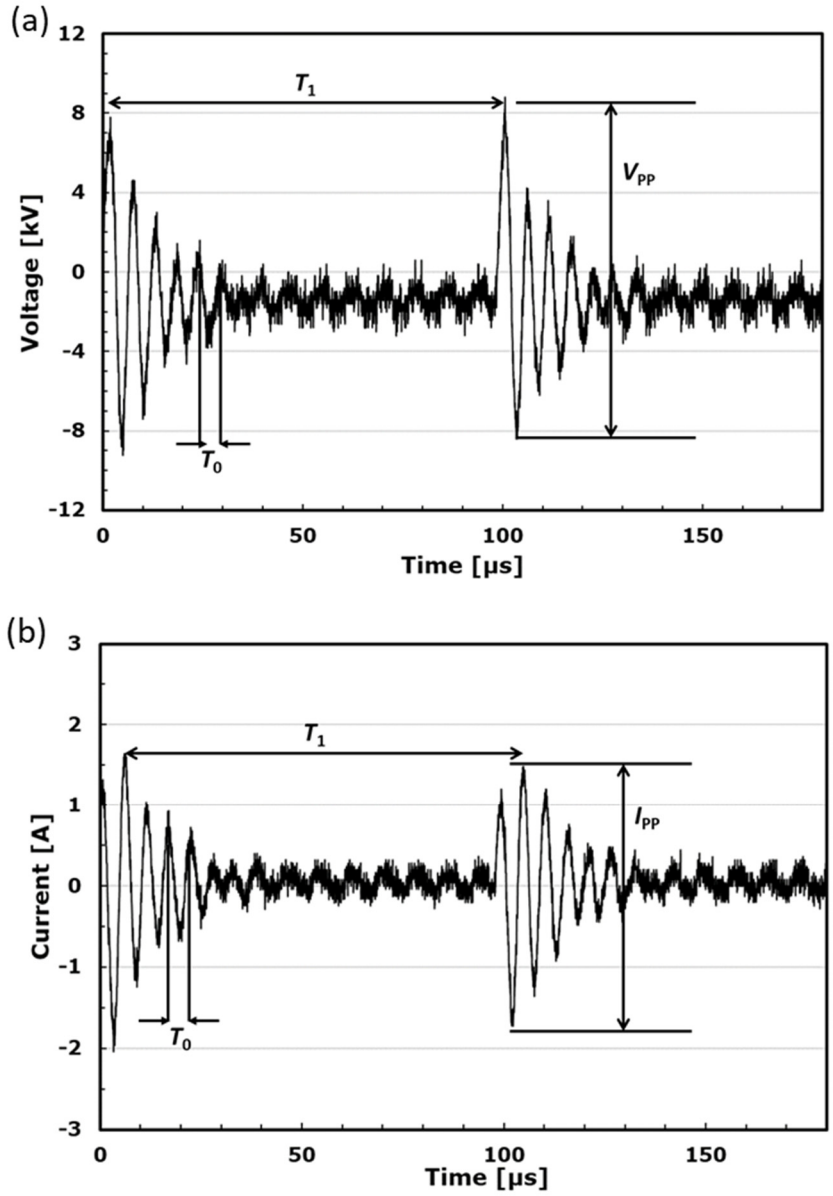


**Fig. 5.** Schematic waveform of (a) voltage and (b) current supplied from a one-cycle sinusoidal power source.

Table 1. lists the experimental conditions for steam decomposition by atmospheric pressure plasma. The boiler has its own pressure setting and is set fixed to 0.2 MPa throughout the study. The supplied steam flow rate was controlled by using a micrometer valve while the $H_2$ concentration was measured with a gas chromatograph (Inficon MicroGC Fusion) at the ice trap outlet. All temperature settings were monitored and controlled through the use of temperature controller (AS ONE, TR-KN-T) and thermocouples.

**Table 1.** Experimental condition for steam decomposition by atmospheric pressure plasma.

| Description | Unit | Value |
|---|---|---|
| **Plasma conditions** | | |
| Pulse Repetition Rate, RR | [kHz] | 10 |
| Applied Voltage | [kV] | 12-18 |
| **For steam decomposition experiment** | | |
| Steam temperature | [°C] | 100-300 |
| Saturated steam flow rate | [mol $min^{-1}$] | 0.250-0.450 |
| Boiler pressure | [MPa] | 0.2 |
| Reactor gap length | [mm] | 0.325, 0.400 |
| Ribbon heater temperature | [°C] | 100-300 |

In the first step of the experiment, the steam flow rate was determined by adjusting the micrometer valve at the exit port of the electric boiler. The steam flowed is then condensed to obtain the mass increased over a period of time, which is then used to calculate the supplied steam flow rate in mL $min^{-1}$ and is converted to mol/min. The steam was flowed from one end of the reactor's gap and travels along the length to exit at the other end of the reactor. The dielectric barrier discharge plasma generated converts the steam molecules into radicals and into hydrogen and oxygen gas. The effect of plasma voltage has been studied in the range of 12 kV to 18 kV. Gases were separated by using the ice trap to condense undecomposed steam into water and separate gas and liquid through their respective outlets. Outlet gases are collected and samples are fed into the gas chromatographer using a 10 mL syringe. Calibration was done on the GC prior to starting the experiment. The gas output flow rate was measured using the displacement tank. Concentration of hydrogen produced was measured and analyzed using gas chromatography. Fig. 6 shows the hydrogen peak alongside oxygen and nitrogen peak detected from the gas sample by the gas chromatographer. The product of total gas output and the hydrogen concentration obtained from the gas chromatography is defined as the hydrogen flow rate (Eqn. 1) while the ratio of the total steam that entered the plasma reactor and the hydrogen obtained is defined as the hydrogen generation rate (Eq. 2). Both rates are calculated by the following equation:

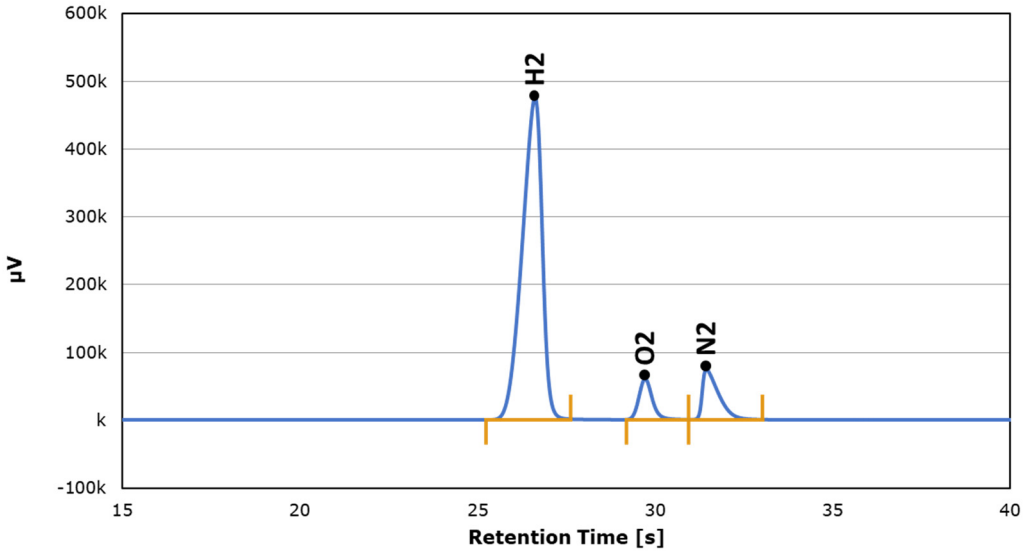


**Fig. 6.** Composition of gas peaks as detected by gas chromatographer from gas sample obtained after steam decomposition.

$$\mathrm{H_2\ Flow\ Rate\ [mol/min]} = H_{2_{Conc}} \times F_{Total\ Gas\ Output} \quad (1)$$

$$\text{H}_2 \text{ Generation Rate } [\%] = (H_2\ Flow\ Rate \div F_{Total\ Steam\ In}) \times 100 \quad (2)$$

The steam decomposition equation can be written as follows [42]:

$$2H_2O \rightarrow 2H_2 + O_2 \quad (3)$$

## 3. Results and discussion

### 3.1 Saturated steam decomposition

First, the hydrogen production from decomposition of saturated steam by atmospheric pressure plasma using a cylindrical plasma reactor was investigated for different supplied steam flow rate and plasma applied voltage.

Fig. 7 shows the graph of generated hydrogen flow rate and hydrogen generation rate against the applied voltage for saturated steam at 100°C. The temperature was kept constant through the use of ribbon heaters and a heating oven. The steam flow rate varied from 0.250 to 0.450 mol $min^{-1}$. Result showed an increase in generated hydrogen with increased supplied steam flow rate. This is attributed to the amount of steam entering the plasma reactor to be decomposed. Increasing the supply flow rate would mean the amount of steam that can be decomposed would also increase.

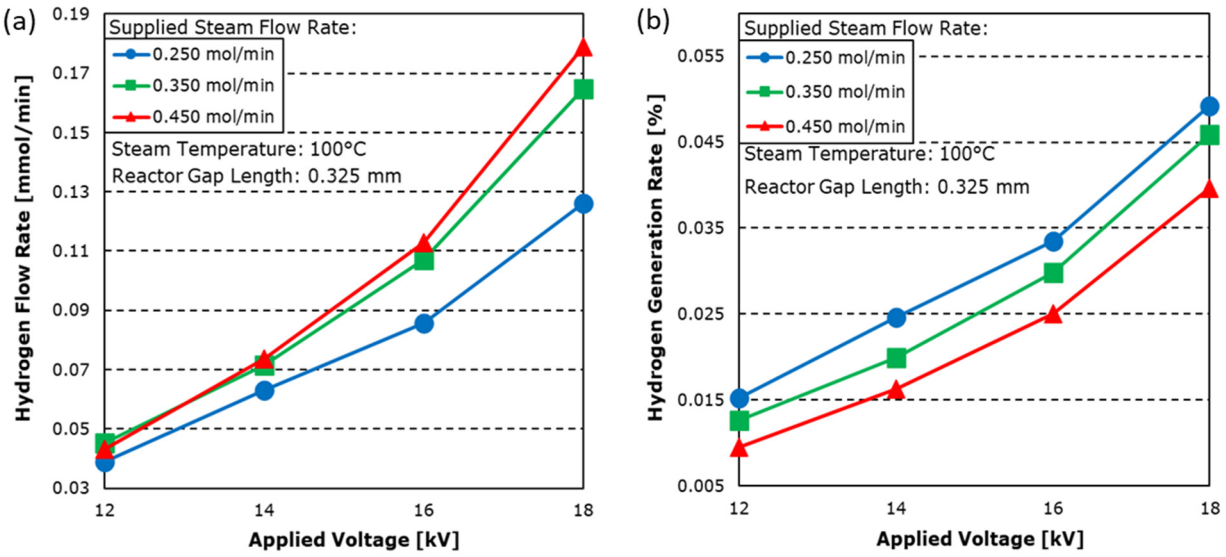


**Fig. 7.** Effect of applied voltage on (a) generated hydrogen flow rate and (b) hydrogen generation rate for saturated steam decomposition.

It can also be seen that the generated hydrogen flow rate and hydrogen generation rate increase with increased applied voltage. Increasing the applied voltage increases electron density which allows steam to decompose easier into H and OH radicals by electron energy [43]. The maximum generated hydrogen flow rate for 0.250, 0.350, and 0.450 mol $min^{-1}$ was 0.126, 0.165, and 0.179 mmol $min^{-1}$ respectively which correspond to a hydrogen generation rate of 0.049%, 0.046%, and 0.040% under the applied voltage of 18 kV. The result also shows that an increased supplied steam flow rate has resulted in a decrease in hydrogen generation rate. This is thought to be attributed to the difference in residence time of steam inside the plasma reactor. The residence time was investigated as a function of the hydrogen generation rate. As shown in Fig. 8, a longer residence time by a lower supplied steam flow rate allows the steam to be properly decomposed compared to a shorter residence time. The residence time is calculated based on the amount of gas flowing into the reactor per unit time and the total volume of the reaction zone and is summarized in the following equation:

$$\text{Residence Time (s)} = \frac{\text{Reactor Volume}}{\text{Total Gas In}} = \frac{\frac{(\text{Gap Length Area} \times \text{Electrode Length})}{10^6}}{\text{Steam Flow Rate} \times \frac{\text{Steam Temperature} + 273.15}{273.15}} \times 60\ s \quad (4)$$

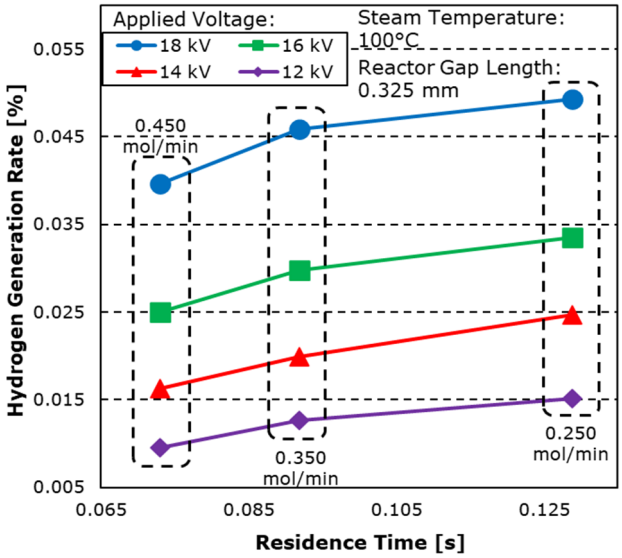


**Fig. 8.** Effect of residence time on the hydrogen generation rate.

The V-I characteristic of the generated plasma has been recorded and the power consumption has been analyzed at various stages of applied voltage. The voltage and current data were used to calculate the power at a time and the overall power consumption was calculated using numerical method of integration. Fig. 9 shows the plasma power consumption along with the hydrogen generation efficiency for applied voltages ranging from 12 kV to 18 kV. The gas flow rate and the steam temperature were fixed at 0.450 mol $min^{-1}$ and 100°C respectively. The result showed that the power consumption increases with increasing applied voltage. The plasma power consumption was highest for 18 kV at 57.73 W. This high energy consumption could be attributed to the formation of water inside of the reactor which acts as an insulator, requiring more power in order to maintain the plasma. The hydrogen generation efficiency was also found to increase with increasing applied voltage. This is related to the increased plasma power which in turn increases steam decomposition rate. The highest hydrogen generation efficiency was 0.186 mmol $Wh^{-1}$ for 18 kV. The average power was used for the efficiency determination. It can be noted that the efficiency could be higher than calculated, as some of the power consumed for plasma is lost to heat and light.

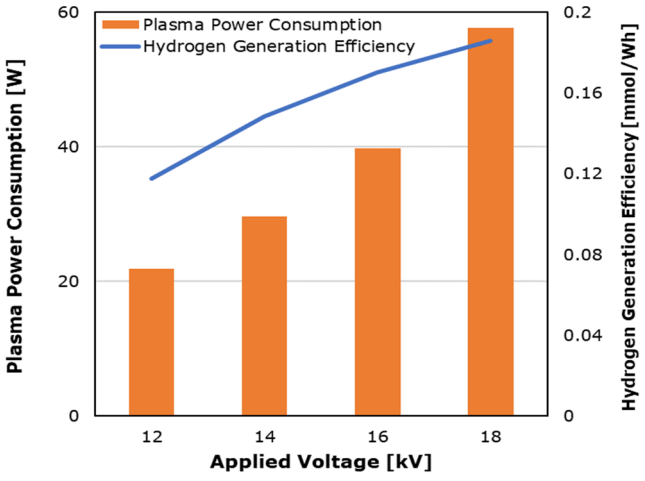


**Fig. 9.** Effect of residence time on the hydrogen generation rate.

## 3.2 Effect of gap length and residence time

In order to further investigate the relationship between the hydrogen generation rate and the residence time, the reactor gap length was increased from 0.325 mm to 0.400 mm while the supplied steam flow rate was kept constant at 0.450 mol $min^{-1}$. Fig. 10 shows the dependency of residence time on the hydrogen generation rate for steam decomposition with different gap length. From the result, it can be seen that the larger reactor volume

of 0.400 mm has helped increase the residence time. This result also showed that longer residence time has an increasing effect on the hydrogen generation rate [44]. Increasing the residence time from 0.073 s to 0.090 s have resulted in an increase of hydrogen generation rate of up to almost 1.5 times from 0.040% to 0.057%. With this in mind, it is thought that increasing the gap length would yield a better hydrogen generation rate. However, increasing the gap length too much would eventually lead to difficulty in plasma firing.

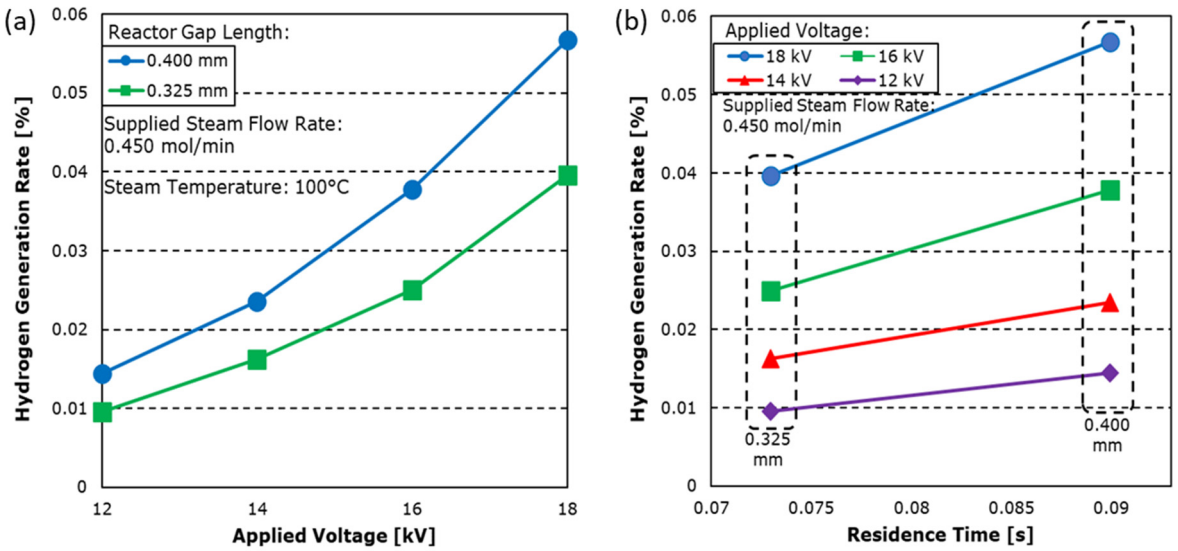


**Fig. 10.** Effect of (a) applied voltage and (b) residence time on hydrogen generation rate for reactor of different gap length.

### 3.3 Hydrogen production mechanics

From the previous result, it is evident that steam decomposition process depends on a number of factors. In order to investigate further the effects on the hydrogen generation rate and overall hydrogen generation process, it is important to understand the steam and plasma conditions and the reactions that are affected by them.

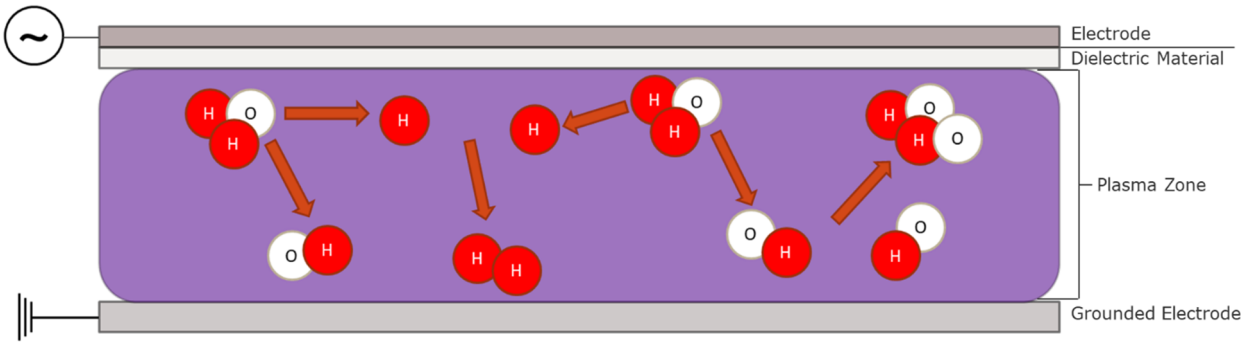


**Fig. 11.** Illustration of hydrogen production mechanics within the plasma reactor.

Fig. 11 shows an illustration of the hydrogen production mechanics within the plasma reactor. Reaction (5) shows the reaction plasma energy collides with the steam molecules and dissociates them into their radicals. From then on, through various collision and energy transfers, the possible reactions and recombination that can be expected is listed below through reactions (6) to (11):

$$e^- + H_2O \rightarrow H + OH + e^- \quad (5)$$

$$OH + H_2 \rightarrow H_2O + H \quad (6)$$

$$H + OH + H_2O \rightarrow 2H_2O \quad (7)$$

$$H + H \rightarrow H_2 \quad (8)$$

$$H + H_2O \rightarrow OH + H_2 \quad (9)$$

$$H + OH \rightarrow H_2 + O \quad (10)$$

$$O + OH \rightarrow O_2 + H \quad (11)$$

$$OH + OH \rightarrow H_2O_2 \quad (12)$$

The possible recombination is assumed to be due to the radicals free flowing around the reactor. As mentioned in the previous section, shorter residence time is thought to have resulted in a lower hydrogen generation rate as steam is not decomposed properly in a short period of time. On the other hand, longer residence time may allow more steam to be decomposed, but it is also possible that the chances of recombination may also increase across different reactions as the free-flowing radicals collide with each other nside the reactor. As can be seen from Fig. 8, it is true that the hydrogen generation rate increases with longer residence time, but it can also be seen that the trendline reaching a peak or even start to decrease after some time. This suggests that there might be an optimum condition in which the hydrogen generation rate is at its highest for steam to be decomposed efficiently.

### 3.4 Effect of steam temperature

Next, the hydrogen generation characteristic of superheated steam is investigated by increasing the supplied steam temperature past 100°C. This is done through the use of an oven furnace which can flash heat the steam to superheated temperatures. In this experiment, the gap length of the reactor and the supplied steam flow rate was kept constant at 0.325 mm and 0.450 mol $min^{-1}$ respectively while the steam temperature was varied from 100°C to 300°C.

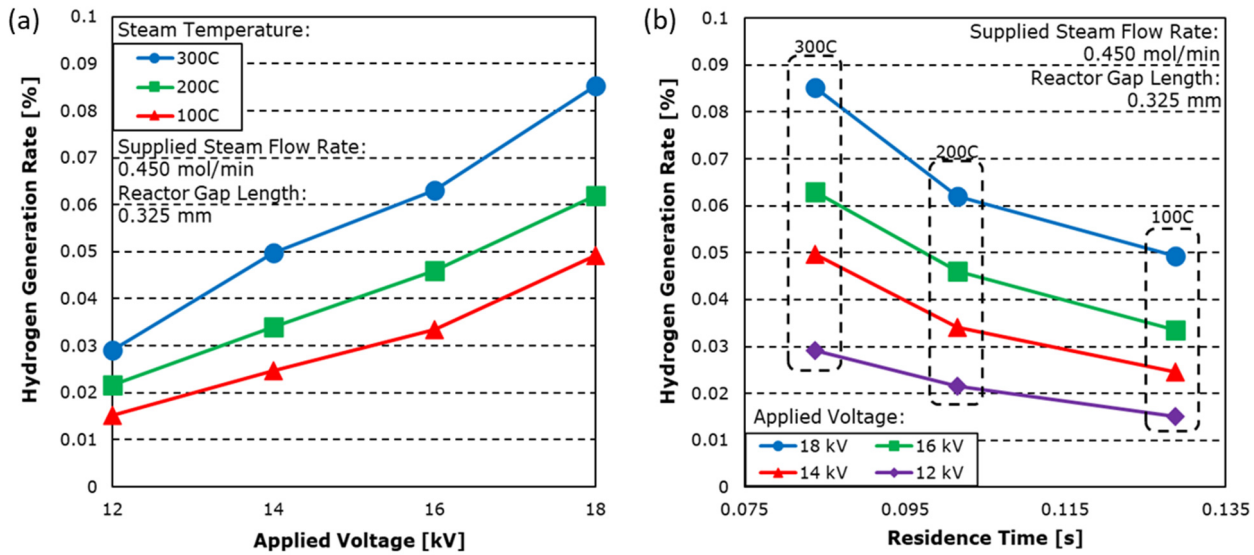


**Fig. 12.** Effect of (a) applied voltage and (b) residence time on hydrogen generation rate for different steam temperatures.

Fig. 12 shows the graph of hydrogen generation rate against applied voltage for different steam temperatures. The result shows that increasing the steam temperature have resulted in an increased hydrogen generation rate. This is possibly due to the existing high thermal energy and conductivity of steam in its superheated state before being decomposed by atmospheric pressure plasma. This is further reflected where steam at 300°C has a shorter residence time than that of steam at 100°C, but has a higher hydrogen generation rate. This may be attributed to the increase in temperature increasing the speed and kinetic energy of steam

molecules in the reactor which resulted in the decrease in residence time. By increasing the temperature from 100°C to 300°C, the hydrogen generation rate was found to increase by almost double from 0.0493% to 0.0853% while the residence time was decreased from 0.129 s to 0.084 s.

## 4. Conclusion

This research aims to develop a hydrogen production system by using a plasma reactor and atmospheric pressure plasma to decompose steam. This study investigated the decomposition characteristics of saturated and superheated steam using a cylindrical type plasma reactor by varying the supplied steam flow rate, reactor gap length, and steam temperature. The result of this study can be used to pave a new way forward for hydrogen generation technologies using atmospheric pressure plasma and water as the source material.

Firstly, decomposition of saturated steam at 100°C was conducted to investigate the feasibility of using water to generate hydrogen using atmospheric pressure plasma. The steam flow rate was supplied using a boiler and the flow rate was determined using a micrometer valve. Results showed an increase in generated hydrogen flow rate with increased applied voltage and supplied flow rate, while hydrogen generation rate only increased with applied voltage and not with supplied flow rate. A hydrogen generation rate of 0.0493% was obtained at an applied voltage of 18 kV and supplied steam flow rate of 0.250 mol $min^{-1}$.

Secondly, the residence time of gas inside the reactor was investigated for its effect on the hydrogen generation rate. The gap length of the reactor was increased from 0.325 mm to 0.400 mm which resulted in a bigger reactor volume and longer residence time. Under the same experimental conditions, the hydrogen generation rate was shown to increase from 0.0396% to 0.0568% for the larger reactor under the same supplied steam flow rate of 0.450 mol/min and at an applied voltage of 18 kV. The hydrogen generation rate was found to depend on the residence time of steam inside the reactor.

Finally, the steam temperature was increased and investigated under superheated temperatures. Different steam temperatures were tested under the same experimental conditions. Under the same supplied steam flow rate and applied voltage, 300°C has shown the highest hydrogen generation rate even though it has the shortest residence time. This is an indication that increased temperature has the capability to help the decomposition of steam using atmospheric pressure plasma. Hydrogen generation rate was shown to increase from 0.0493% to 0.0853% with a difference in residence time of 45 ms.

## Acknowledgment

The authors would like to thank Mr. Shigeo Takitani and Mr. Tomokazu Kodera from Kawada Industries, Ltd for providing experimental equipment and support.

## References

[1] Dincer I., and Acar, C., Smart energy solutions with hydrogen options, *Int. J. Hydrog. Energy*, Vol. 43 (18), pp. 8579–8599, 2018.

[2] Mathiesen B.V., and Lund H., Comparative analyses of seven technologies to facilitate the integration of fluctuating renewable energy sources, *IET Renewable Power Generation*, Vol. 3 (2), pp. 190–204, 2009.

[3] Zhang Z., Liguori S., Fuerst T.F., Way J.D., and Wolden C. A., Efficient ammonia decomposition in a catalytic membrane reactor to enable hydrogen storage and utilization, *ACS Sustain. Chem. Eng.*, Vol. 7 (6), pp. 5975–5985, 2019.

[4] Kumar S.S., and Himabindu, V., Hydrogen production by PEM water electrolysis–A review, *Materials Sci. Energy Technol.*, Vol. 2 (3), pp. 442–454, 2019.

[5] Martins F., Felgueiras C., and Smitková M., Fossil fuel energy consumption in European countries. *Energy Procedia*, Vol. 153, pp. 107–111, 2018.

[6] Ritchie H., and Roser M., Fossil fuels. *Our world in data*., 2017.

[7] Bououdina C., and Guo Z. X., Carrying clean energy to the future–hydrogen absorbing materials, *Mater. Technol*., Vol. 15 (4), pp. 269–275, 2000.

[8] Cha J., Jo Y. S., Jeong H., Han J., Nam S. W., Song K. H., and Yoon C. W., Ammonia as an efficient $CO_X$-free hydrogen carrier: Fundamentals and feasibility analyses for fuel cell applications, *Appl. Energy*, Vol. 224, pp. 194–

204, 2018.
[9] Hosseini, S. E., and Wahid, M. A., Hydrogen from solar energy, a clean energy carrier from a sustainable source of energy, *Int. J. Energy Res.*, Vol. 44 (6), pp. 4110–4131, 2020.
[10] Chapman A., Itaoka K., Farabi-Asl H., Fujii Y., and Nakahara M., Societal penetration of hydrogen into the future energy system: Impacts of policy, technology and carbon targets, *Int. J. Hydrog. Energy*, Vol. 45 (7), pp. 3883–3898, 2020.
[11] Jain I. P., Hydrogen the fuel for 21st century, *Int. J. Hydrog. Energy*, Vol. 34 (17), pp. 7368–7378, 2009.
[12] Ursua A., Gandia L. M., and Sanchis P., Hydrogen production from water electrolysis: current status and future trends, *Proc. IEEE*, Vol. 100 (2), pp. 410–426, 2011.
[13] Chehade G., Lytle S., Ishaq H., and Dincer I., Hydrogen production by microwave based plasma dissociation of water. *Fuel*, Vol. 264, 116831, 2020.
[14] Rehman F., Lozano-Parada J. H., and Zimmerman W. B., A kinetic model for $H_2$ production by plasmolysis of water vapours at atmospheric pressure in a dielectric barrier discharge microchannel reactor, *Int. J. Hydrog. Energy*, Vol. 37 (23), pp. 17678–17690, 2012.
[15] Chandrasekhar K., Kumar S., Lee B. D., and Kim S. H., Waste based hydrogen production for circular bioeconomy: Current status and future directions. *Bioresour. Technol.*, Vol. 302, 122920, 2020.
[16] Kalamaras C. M., and Efstathiou A. M., Hydrogen production technologies: current state and future developments, *Conference Papers in Science*, Vol. 2013, 690627, 2013.
[17] Acar C., and Dincer I., Comparative assessment of hydrogen production methods from renewable and non-renewable sources, *Int. J. Hydrog. Energy,* Vol. 39 (1), pp. 1–12, 2014.
[18] Dincer, I., and Acar, C., Review and evaluation of hydrogen production methods for better sustainability, *Int. J. Hydrog. Energy*, Vol. 40 (34), pp. 11094–11111, 2015.
[19] Ju Li, Cunhua Ma, Shengjie Zhu, Feng Yu, Bin Dai, and Dezheng Yang, A Review of Recent Advances of Dielectric Barrier Discharge Plasma in Catalysis, Nanomaterials (Basel). 2019.
[20] Tochikubo F., Fundamentals of atmospheric pressure plasma, *J. Institute Electrical Eng. Jpn*., Vol. 126 (12), pp. 781–783, 2006.
[21] Dey G. R., and Das T. N., Yields of hydrogen and hydrogen peroxide from argon–water vapor in dielectric barrier discharge, *Plasma Chem. Plasma Proc*., Vol. 36 (2), pp. 523–534, 2016.
[22] Akiyama M., Aihara K., Sawaguchi T., Matsukata M., and Iwamoto M., Ammonia decomposition to clean hydrogen using non-thermal atmospheric-pressure plasma, *Int. J. of Hydrog. Energy*, Vol. 43 (31) pp. 14493–14497, 2018.
[23] Chen F., Huang, X., Cheng, D.G., and Zhan,X., Hydrogen production from alcohols and ethers via cold plasma: A review, *Int. J. Hydrogen Energy*, Vol. 39 (17), pp. 9036–9046, 2014.
[24] Lamb K.E., Dolan M.D., and Kennedy, D. F., Ammonia for hydrogen storage; A review of catalytic ammonia decomposition and hydrogen separation and purification, *Int. J. Hydrogen Energy*, Vol. 44 (7), pp. 3580–3593, 2019.
[25] Varne M., Dey G. R., and Das T.N., Evaluation of optimum conditions for hydrogen generation in argon-water vapor dielectric barrier discharge, *Int. J. Hydrog. Energy*, Vol. 41 (48), pp. 22769–22774, 2016.
[26] Chen X., Marquez M., Rozak, J., Marun C., Luo J., Suib S. L., Hayashi Y., and Matsumoto H., $H_2O$ splitting in tubular plasma reactors, *J. Cat.*, Vol. 178 (1), pp. 372–377, 1998.
[27] Jung Y. H., Jang S. O., and You H. J., Hydrogen generation from the dissociation of water using microwave plasmas, *Chinese Phys. Lett.*, Vol. 30 (6), 065204, 2013.
[28] Ong Kok S., Liben Jiang, and Koon C. L., Thermoelectric energy conversion, *Comprehensive Energy Systems*, Vol. 4, pp. 794–815, 2018.
[29] Woolley E., Luo Y., and Simeone A., Industrial waste heat recovery: A systematic approach, *Sustain. Energy Technol. Assess.*, Vol. 29, pp. 50–59, 2018.
[30] Papapetrou M., Kosmadakis G., Cipollina A., La Commare U., and Micale G., Industrial waste heat: Estimation of the technically available resource in the EU per industrial sector, temperature level and country, *Appl. Thermal Eng*., Vol. 138, pp. 207–216, 2018.
[31] Haddad C., Périlhon C., Danlos A., François M. X., and Descombes G., Some efficient solutions to recover low and medium waste heat: competitiveness of the thermoacoustic technology, *Energy Procedia*, Vol. 50, pp. 1056–1069, 2014.
[32] Jouhara H., Khordehgah N., Almahmoud S., Delpech B., Chauhan A., and Tassou S. A., Waste heat recovery technologies and applications, *Thermal Sci. Eng. Progress*, Vol. 6, pp. 268–289, 2018.
[33] Brückner S., Liu S., Miró L., Radspieler M., Cabeza L. F., and Lävemann E., Industrial waste heat recovery technologies: An economic analysis of heat transformation technologies, *Applied Energy*, Vol. 151, pp. 157–167, 2015.
[34] Xu Z. Y., Wang R. Z., and Yang C., Perspectives for low-temperature waste heat recovery, *Energy*, Vol. 176, pp. 1037–1043, 2019.
[35] Barker G. B., The engineer's guide to plant layout and piping design for the oil and gas industries, Gulf Professional Publishing, 2017.

[36] Yamada O., Generation of hydrogen gas by reforming biomass with superheated steam, *Thin Solid Films*, Vol. 509 (1–2), pp. 207–211, 2006.
[37] Tetsuya Kadoma, Takushi Kishimoto, Motoki Tanaka, Seiji Takami, Development of healthy cooking technology with superheated steam, *J. Cookery Sci. Jpn*., Vol. 39 (2), pp. 163–166, 2006.
[38] Sehrawat R., Nema P. K., and Kaur B. P., Effect of superheated steam drying on properties of foodstuffs and kinetic modeling, *Innovative Food Sci. Emerging Technol.*, Vol. 34, pp. 285–301, 2016.
[39] Noburou Osa, Superheated Steam: A promising prospect, overview of superheated steam, Serial Lecture No. 195, 2014.
[40] Kambara S., Hayakawa Y., Inoue Y., and Miura T., Hydrogen production from ammonia using plasma membrane reactor, *J. Sustain. Dev. Energy Water Environ. Syst.*, Vol.4 (2), pp. 193–202, 2016.
[41] Hayakawa Y., Miura T., Shizuya K., Wakazono S., Tokunaga K., and Kambara S., Hydrogen production system combined with a catalytic reactor and a plasma membrane reactor from ammonia, *Int. J. Hydrogen Energy*, Vol. 44 (20), pp. 9987–9993, 2019.
[42] Lukes P., Clupek M., Babicky V., Simek M., Tothova I., Janda V., Moucha T, and Kordac M., Role of solution conductivity in the electron impact dissociation of $H_2O$ induced by plasma processes in the pulsed corona discharge in water. In *HAKONE XI, 11th International Symposium on High Pressure, Low Temperature Plasma Chemistry,* Contributed Papers, Oleron Island, 2008.
[43] Rehman F., Abdul Majeed W. S., and Zimmerman W. B., Hydrogen production from water vapor plasmolysis using DBD-Corona hybrid reactor, *Energy Fuels*, Vol. 27 (5), pp. pp. 2748–2761, 2013.
[44] Jimenez M., Rincon R., Marinas A., and Calzada M. D., Hydrogen production from ethanol decomposition by a microwave plasma: Influence of the plasma gas flow, *Int. J. Hydrogen Energy*, Vol. 38 (21), pp. 8708–8719, 2013.